Advanced Control for Quadruple Tank Process

Iput Kasiyanto[1], Himma Firdaus[1], Qudsiyyatul Lailiyah[1], Ihsan Supono[1], Nanang Kusnandar[1], Ihsan Supono[2]

[1]National Research and Innovation Agency (BRIN)

[2]Universitas Pamulang

ARTICLE INFO

ABSTRACT

In the realm of control systems, the last three decades have witnessed significant advancements in Model Predictive Control MPC), an advanced technique renowned for its ability to optimize processes with constraints, handle multivariate systems, and incorporate future references when feasible. This paper introduces an innovative offset-free MPC approach tailored for the control of a complex nonlinear system—the Quadruple Tank Process (QTP). The QTP, known for its deceptively simple yet challenging multivariate behavior, serves as an ideal benchmark for evaluating the efficacy of the proposed algorithm. In this work, we rigorously compare the performance of the PID and MPC controller when applied to both linear and nonlinear models of the QTP. Notably, our research sheds light on the advantages of MPC, particularly when confronted with constant disturbances. Our novel algorithm demonstrates exceptional capabilities, ensuring error-free tracking even in the presence of persistent load disturbances for both linear and nonlinear QTP models. Compared to the PID control, the proposed method can reduce the overall set point tracking error up to 32.1%, 27.6%, and 38.54% using the performance indices ISE, ITAE, and IAE, respectively, for the linear case. Furthermore, for the nonlinear case, the overall set point tracking error reduction is up to 93.4%, 94.9%, and 91.5%. This work contributes to bridging the gap in effective control strategies for nonlinear systems like the QTP, highlighting the potential of offset-free MPC to enhance control and stability in a challenging process industry involving automatic liquid level control.

Corresponding Author:

Iput Kasiyanto, National Research and Innovation Agency (BRIN)
Email: iput003@brin.go.id

1. INTRODUCTION

Over the past three decades, Model Predictive Control (MPC), an advanced control technique, has undergone significant development, finding applications extensively in both academia and industry [1], [2]. MPC offers a powerful solution to constrained control problems, featuring optimal control, and the management of coupled and multivariable processes. With its origins in the petrochemical industry, MPC has evolved through contributions from academia, maturing its theoretical foundations and demonstrating effectiveness in diverse industrial applications [3], [4].

While MPC has proven its robustness and stability in the presence of disturbances and uncertainties, achieving offset-free control often necessitates integral action, a feature found in traditional controllers like PI/PID. Integrating integral action into MPC designs typically involves observers to estimate disturbances and adapt the system's states accordingly [5], [6]. However, it's important to consider that the inclusion of state and uncertainty estimation doesn't guarantee zero-offset tracking control [7]. An alternative approach, as proposed by Hermansson and Syafiie [8], combines multiple model predictive controllers and includes adaptive integral action control.

This article introduces an offset-free model predictive control (MPC) method tailored for the servo and regulatory action of a nonlinear system—the quadruple tank process (QTP). The QTP, initially introduced by Johansson [9], remains a classical benchmark control problem due to its multivariable and nonlinear nature

[10], [11]. This process is very suitable to demonstrate performance limitations in multivariable control design due to right half-plane zeros. The QTP can be considered as a prototype of many industrial applications in the process industry involving liquid level control such as chemical and petrochemical plants [12]. Previous research has explored various control strategies for the QTP, including decentralized PI/PID controllers [9], [10], [13]–[21], fractional order PI control [22]–[25], Model Reference Adaptive Controller (MRAC) [13], [26], state error feedback linearization control method with disturbance observer (DOB) and L_2 gain [27]–[30], low-gain integral controllers [31], generalized predictive control (GPC) [32], and sliding mode control [12], [23], [33]–[37], optimal control [38]–[40], and intelligent control techniques [21], [39], [41]–[49].

The primary objective of this study is to develop an MPC approach that achieves error-free tracking for the QTP, both for linear and nonlinear cases. Furthermore, for a more obvious understanding, this study also compares the performance of the MPC with a decentralized PID control. Distinguishing itself from prior works that employed conventional controllers [9], [10], [14], or multiple MPCs [8], our approach deploys a single MPC.

Since automatic liquid level regulation is crucial in process industries, an effective and efficient control method is a requirement. The dynamics of QTP resembles that of many real systems such as boiler process, distillation column, oil refineries in petrochemical industries, and many more. These processes involve an interacting tank system that is difficult to control. By addressing the challenge of offset-free tracking for the QTP using MPC, this research aims to contribute to the field of control systems while providing practical insights for real-world applications.

The outline of this article is presented as follows. The first part of Section 2 provides an overview of the QTP and presents a linear model for control design. Then, we will explain the PID controller design concisely in the second part of Section 2. Subsequently, the section will be closed with a thorough elaboration on the MPC design, including a novel error-tracking strategy. Section 3 compares the control performance of the PID and the MPC controllers both for the linear and nonlinear QTP models. This section will also evaluate MPC's robustness to constant disturbances. Finally, Section 4 summarizes the findings and conclusions drawn from the simulation results.

2. RESEARCH METHODS
2.1. Quadruple Tank Process
In this section, a concise overview of the QTP will be described. Then, a linear model derivation for control design is presented.

2.2. System Description
This section will derive a mathematical model for the quadruple tank process (QTP). The QTP consists of four interconnected water tanks and two dedicated pumps [9]. The schematic drawing of the QTP is provided in Fig. 1.
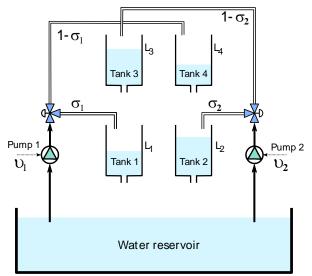

Fig. 1. Schematic diagram of QTP.

Water is delivered from the reservoir to both the upper and the lower tanks. Pump 1 transfers water to tanks 1 and 4, while pump 2 supplies water to tanks 2 and 3. The manipulated variables of the QTP are the voltages applied to the pumps, denoted as v_1 and v_2 [V]. The controlled variables are the water levels of the two lower tanks, denoted as L_1 and L_2 [cm]. The split ratio σ is determined by the valve positions. Let's assume that the states of the system are the water levels of tank 1 to tank 4, denoted as $L_1, L_2, L_3,$ and L_4 respectively. It should be noted that all continuous variables are time-dependent, but for simplicity, time indices have been omitted. For instance, the level variable is denoted by $L_i(t) := L_i \, for \, i = 1, ... ,4$. The dynamics of the system are derived using first principles, i.e., mass balances and Bernoulli's law as follows

$$\frac{dL_1}{dt} = -\frac{\alpha_1}{A_1}\sqrt{2gL_1} + \frac{\alpha_3}{A_1}\sqrt{2gL_3} + \frac{\sigma_1\kappa_1}{A_1}v_1$$

$$\frac{dL_2}{dt} = -\frac{\alpha_2}{A_2}\sqrt{2gL_2} + \frac{\alpha_4}{A_2}\sqrt{2gL_4} + \frac{\sigma_2\kappa_2}{A_2}v_2$$

$$\frac{dL_3}{dt} = -\frac{\alpha_3}{A_3}\sqrt{2gL_1} + \frac{(1-\sigma_2)\kappa_2}{A_3}v_2 \qquad (1)$$

$$\frac{dL_4}{dt} = -\frac{\alpha_4}{A_4}\sqrt{2gL_4} + \frac{(1-\sigma_1)\kappa_1}{A_4}v_1$$

where L_1 is the water level [cm], α_i is the cross-section area of the outlet hole [cm^2], $A_2 (i = 1, ... ,4)$ is the corresponding tank's cross-sectional area [cm^2]. Additionally, v_1 and v_2 are the applied voltage to the pump [V]; whereas σ_1 and σ_2 denote the split ratio of valves 1 and 2; κ_1 and κ_2 are constants that signify the relationship between the control voltages and the pumps' water flow [cm^3/Vs], g is the gravitational constant [cm/s^2], and κ_c is a constant associating the voltage and the tank level [V/cm]. The values of the system parameters can be found in Table 1.

Table 1. Numerical values of the QTP system parameter

Parameter	Value	Unit
α_1, α_3	0.081	cm^2
α_2, α_4	0.067	cm^2
κ_1, κ_2	3.33, 3.35	cm^3/Vs
κ_c	0.50	v/cm
A_2, A_4	40	cm^2
A_1, A_3	30	cm^2
g	981	cm/s^2

2.3. Linear Model

According to Johansson [9], the QTP has a unique feature that makes it popular as a benchmark for control strategy proposals, i.e. having an adjustable transmission zero in its linear system. The zero location varies from the left half to the right half of the s-plane based on the split ratio value. Changing the split ratio σ_1 and σ_2 allows a zero with a negative real part, which corresponds to the minimum phase mode. In this mode, the flow to the lower tanks is greater than the flow to the upper tanks, specifically $1 < \sigma_1 + \sigma_2 < 2$. On the contrary, if the linear model has a zero with a positive real part, then it corresponds to the non-minimum phase (NMP) mode. In this mode, the flow to the lower tanks is smaller than the flow to the upper tanks, specifically $0 < \sigma_1 + \sigma_2 < 1$. In this study, the valve positions σ_i are set in a way that an NMP system is achieved. Thus, we choose $\sigma_1 = 0.25$ and $\sigma_2 = 0.35$. Of course, controlling an NMP system is harder than the minimum one. This can be understood since more fluid flows into the two upper tanks than into the two bottom tanks yielding competing effects between the initial and steady-state system responses. This attribute, alongside constraints and a multivariate nature, can deteriorate closed-loop system performance, even worse leading to instability [50].

Since the process described in (1) is nonlinear, creating a linear model to utilize the MPC algorithm is necessary. By defining $\boldsymbol{L}, \boldsymbol{y}, \boldsymbol{v}, \boldsymbol{L}^0, \boldsymbol{y}^0,$ and $\boldsymbol{v}^0$ vectors as $\boldsymbol{L} = [L_1 \quad L_2 \quad L_3 \quad L_4]^T$, $\boldsymbol{y} = [L_1 \quad L_2]^T$, $\boldsymbol{v} = [v_1 \quad v_2]^T$, $\boldsymbol{L}^0 = [L_1^0 \quad L_2^0 \quad L_3^0 \quad L_4^0]^T$, $\boldsymbol{y}^0 = [L_1^0 \quad L_2^0]^T$ and $\boldsymbol{v}^0 = [v_1^0 \quad v_2^0]^T$, respectively. Then, by introducing $\Delta \boldsymbol{L} := \boldsymbol{L} - \boldsymbol{L}^0$, $\Delta \boldsymbol{v} := \boldsymbol{v} - \boldsymbol{v}^0$ and $\Delta y := \boldsymbol{y} - \boldsymbol{y}^0$, the linearized QTP model is obtained as follows

$$\frac{d}{dt}(\Delta \boldsymbol{L}) = \begin{bmatrix} -\dfrac{1}{\Gamma_1} & 0 & \dfrac{A_4}{A_1\Gamma_3} & 0 \\ 0 & -\dfrac{1}{\Gamma_2} & 0 & \dfrac{A_4}{A_2\Gamma_4} \\ 0 & 0 & -\dfrac{1}{\Gamma_3} & 0 \\ 0 & 0 & 0 & -\dfrac{1}{\Gamma_4} \end{bmatrix} \Delta \boldsymbol{L} + \begin{bmatrix} \dfrac{\sigma_1\kappa_1}{A_1} & 0 \\ 0 & \dfrac{\sigma_2\kappa_2}{A_2} \\ 0 & \dfrac{(1-\sigma_2)\kappa_2}{A_3} \\ \dfrac{(1-\sigma_1)\kappa_1}{A_4} & 0 \end{bmatrix} \Delta \boldsymbol{v} \tag{2}$$

$$\Delta \boldsymbol{y} = \begin{bmatrix} \kappa_c & 0 & 0 & 0 \\ 0 & \kappa_c & 0 & 0 \end{bmatrix} \Delta \boldsymbol{L}$$

where the time constants Γ_i are defined as

$$\Gamma_i = \frac{A_i}{\alpha_i}\sqrt{\frac{2L_i^0}{g}}, \quad i = 1, \dots, 4 \tag{3}$$

and the corresponding transfer matrix is

$$G_p(s) = \begin{bmatrix} \dfrac{\beta_1\sigma_1}{1+s\Gamma_1} & \dfrac{(1-\beta_2)\sigma_1}{(1+s\Gamma_1)(1+s\Gamma_3)} \\ \dfrac{(1-\beta_1)\sigma_2}{(1+s\Gamma_2)(1+ss\Gamma_4)} & \dfrac{\beta\tau_2\sigma_2}{1+s\Gamma_2} \end{bmatrix} \tag{4}$$

where $\beta_1 = \kappa_c\kappa_1\Gamma_1/A_1$ and $\beta_2 = \kappa_c\kappa_2\Gamma_2/A_2$.
The corresponding operating conditions, L_1^0 and v_1^0, are given in Table 2.

Table 2. The operating condition values for the NMP QTP ($\sigma_1 = 0.25$ and $\sigma_2 = 0.35$)

Variables	Value	Unit
L_1^0, L_2^0	8.62, 18.7	cm
L_3^0, L_4^0	4.51, 8.67	cm
v_1^0, v_2^0	3.5, 3.5	V

Using (3), (4), and the parameter values given in Table 1 and Table 2, the following time constants and transfer function matrix are obtained

$$\Gamma_1 = 49.1\ s, \quad \Gamma_2 = 116.7\ s, \quad \Gamma_3 = 35.5\ s, \quad \Gamma_4 = 79.4\ s$$

$$G_p(s) = \begin{bmatrix} \dfrac{0.68}{1+49.1s} & \dfrac{1.77}{(1+49.1s)(1+35.5s)} \\ \dfrac{3.66}{(1+116.7s)(1+79.4s)} & \dfrac{1.71}{1+116.7s} \end{bmatrix} \tag{5}$$

Fig. 2 shows simulations of the NMP model compared to the nonlinear model described by (1). The inputs are random sequences with amplitudes of $v_{1,2} \in [2,5]$, so that the linear model can capture the nonlinear dynamics. As the goodness of fit measure between the linear NMP model and the nonlinear process, we use root mean squared error (RMSE) as commonly expressed in (6).

$$e_M = \sqrt{\sum_{j=1}^{n} \frac{(\hat{y}_j - y_j)^2}{n}} \tag{6}$$

where $\hat{y}_j$ is the j-th model data, y is the j-th reference data, and n is the number of the samples.

For this particular case, the e_M is 0.1384 and 0.4614 for L_1 and L_2, respectively. It indicates that the linear model agrees well with the responses of the nonlinear QTP. Additionally, the transmission zeros are

$z = (-0.066, 0.025)$ for this particular case. Note that one of the transmission zeros has a positive value, which indicates that the corresponding system in (5) is indeed an NMP system.
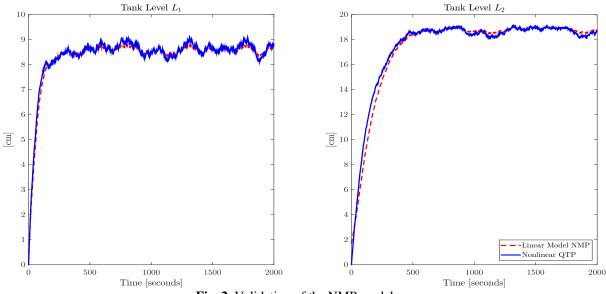

Fig. 2. Validation of the NMP model.

2.4. PID Controller Design

This section will discuss a decentralized PID controller design for a multivariable system, studied by many researchers, see [9], [10], [13]–[21] for instance. But, before delving into PID control design, a brief overview of the relative gain array (RGA) will be described and analyzed.

2.5. Relative Gain Array (RGA)

When dealing with a coupled multivariable control system, the notion of RGA is very important since it is a measure of the interaction nature among the elements of the multivariable system. In the process industry, the RGA is the main tool for deciding on control structure problems, specifically input-output pairing for decentralized controllers. The common formula to compute the RGA μ is $\mu = G_p(0) * G_p^{-T}(0)$, where the asterisk denotes element-by-element matrix multiplication and $-T$ inverse transpose. Using the formula, the obtained RGA μ is

$$\mu = \begin{bmatrix} -0.22 & 0.59 \\ 2.52 & -0.22 \end{bmatrix}$$

The non-zero values in the off-diagonal elements indicate that the multivariable system has an interacting nature with each other. But for the QTP, the following simple expression can be used to calculate the RGA [9]

$$\mu = \frac{\sigma_1 \sigma_2}{\sigma_1 + \sigma_2 - 1} \tag{7}$$

Note that the RGA only depends on the split ratio $\sigma_{1,2}$ settings. For $\sigma_1 = 0.25$ and $\sigma_2 = 0.35$, then we get $\mu = -0.0959$. This indicates that the system is hard to control because of the value of $\mu < 0$ [9].

2.6. PID Controller Structure

In this section, a decentralized PID controller will be designed. As indicated in the previous section, the NMP QTP indeed owes an interaction problem between the neighboring process variables. The common method to solve the problem is to employ the decoupling technique in the control structure. Many authors proposed methods to determine the decoupler matrix, see in [14], [17], [18], [20].

A parallel form of PID is used in this study. The transfer function for each controller can be expressed in s-domain as follows

$$C_{PID}(s) = K_p + \frac{K_i}{s} + K_d \frac{s}{T_f \cdot s + 1} \tag{8}$$

where K_p, K_i, and K_d are the proportional, integral, and derivative gains, respectively; T_f is the derivative filter time. The schematic diagram for the PID controller is given in Fig. 3. $C_1(s)$ and $C_2(s)$ are the PID controllers for loop 1 and loop 2, respectively. ξ_i is the input disturbance to each controller. $r_1(s)$ and $r_2(s)$ are the reference signals.
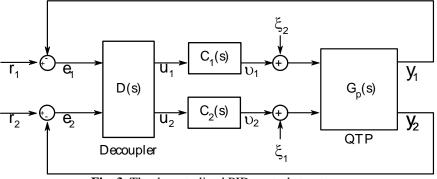

Fig. 3. The decentralized PID control structure.

Using Matlab/Simulink and Control System toolboxes, the following static decoupler matrix and PID's tuning parameters are employed in this work

$$D(s) = \begin{bmatrix} 0.948 & 1.989 \\ 3.439 & 2.442 \end{bmatrix}$$

$$K_{p1} = 1.893, \quad K_{i1} = 0.011, \quad K_{d1} = 75, \quad T_{f1} = 0.043 \tag{9}$$

$$K_{p2} = 2.457, \quad K_{i2} = 0.0286, \quad K_{d2} = 37.056, \quad T_{f2} = 0.031$$

2.7. Model Predictive Control (MPC) Design

Having derived a mathematical model and PID control design for the QTP in the previous section, a brief overview of MPC and its design steps will be elaborated in this section. Model predictive control (MPC) is a sophisticated control method that can naturally manage multiple-input multiple-output (MIMO) processes and take constraints into account explicitly [51]. The MPC converts the control system problem into an optimization formulation. By using an identified model, it solves an open-loop optimal control problem (OCP) iteratively in a finite horizon at every sampling time to obtain the control action sequences. However, only the first control action is implemented while the remainder is omitted [52], [53]. Then, the procedure is repeated for the next sample instant after shifting the horizon one step ahead. Thus, the MPC is sometimes called receding horizon control.

2.8. State space Model

Since MPC is a model-based control strategy, one should provide a model to make use of the approach. In this work, a linear model in the form of state space is assumed to be available. The subsequent equation denotes a linear time-invariant (LTI), discrete system:

$$
\begin{aligned}
x(k + 1) &= Ax(k) + Bu(k) \\
y(k) &= C_y x(k) \\
z(k) &= C_z x(k) + D_z u(k) \\
z_c(k) &= C_c x(k) + D_c u(k)
\end{aligned}
\tag{10}
$$

where $u(k) \in R^m$ is the control input vector, $x(k) \in R^n$ the state vector, $y(k) \in R^{P_y}$ the measured output, and $z(k) \in R^{P_z}$ is the controlled output vector. One of the benefits possessed by MPC is that it can consider constraints not only on the control variables $u(k)$ but also on the constrained outputs $z_c(k) \in R^{p_c}$ as formulated in (11):

$$\Delta \boldsymbol{u}_{min} \leq \Delta \boldsymbol{u}(k) \leq \Delta \boldsymbol{u}_{max}, \quad k \in I_u$$
$$\boldsymbol{u}_{min} \leq \boldsymbol{u}(k) \leq \boldsymbol{u}_{max}, \quad k \in I_u \tag{11}$$
$$\boldsymbol{z}_{min} \leq \boldsymbol{z}_c(k) \leq \boldsymbol{z}_{max}, \quad k \in I_p$$

The control increment $\Delta \boldsymbol{u}(k)$ above is defined as $\Delta \boldsymbol{u}(k) = \boldsymbol{u}(k) - \boldsymbol{u}(k-1)$. I_p and I_u are the blocking factors (see § Blocking Factor) for the controlled and control variables, respectively. Note that the controlled and constrained variables in (10) are separated. This formula is to accommodate cases where the reference values are only available for the controlled variables, but not for the constrained ones.

2.9. Optimal Control Problem

The essence of the MPC control method can be seen in how it formulates an OCP. Consider a quadratic cost function as follows

$$J(k) = \sum_{i=L_w}^{L_p+L_w-1} \|\hat{\boldsymbol{z}}(k+i|k) - \boldsymbol{r}(k+i|k)\|_{\boldsymbol{Q}(i)}^2 + \sum_{i=0}^{L_u-1} \|\Delta \hat{\boldsymbol{u}}(k+i|kk)\|_{\boldsymbol{R}(i)}^2 \tag{12}$$

where $\hat{\boldsymbol{z}}(k+i|k)$ and $\Delta \hat{\boldsymbol{u}}(k+i|k)$ are the predicted controlled output and the predicted control input increments sequence at time k. In addition, the symmetric weighting matrices $\mathbf{Q} \geq \mathbf{0}$ and $\mathbf{R} > \mathbf{0}$ are assumed to be constant over the prediction horizon L_p. Note that the first sample included in the horizon is indicated by L_w. Further, the control horizon is denoted by L_u. Also, notice that in (12) $\Delta \boldsymbol{u}(k)$ is penalized instead of $\boldsymbol{u}(k)$. This is a common practice in linear quadratic control.
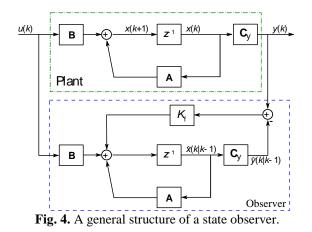
2.10. State Estimation

The need for state estimation arises since often there is a case where the present state is not available. For a plant described as

$$\boldsymbol{x}(k+1) = \boldsymbol{A}\boldsymbol{x}(k) + \boldsymbol{B}\boldsymbol{u}(k)$$
$$\boldsymbol{y}(k) = \boldsymbol{C}_y\boldsymbol{x}(k), \tag{13}$$

we can make use of a state observer, as shown in Fig. 4, to estimate the unknown state variables.

Fig. 4. A general structure of a state observer.

The observer is a copy of the plant, using feedback from the measured output, to obtain the state estimate $\hat{\boldsymbol{x}}(k)$. The underlying principle of the observer is governed by the following equations

$$\hat{\boldsymbol{x}}(k|k) = \hat{\boldsymbol{x}}(k|k-1) + \boldsymbol{K}_f^T \big(\boldsymbol{y}(k) - \hat{\boldsymbol{y}}(k|k-1)\big)$$
$$\hat{\boldsymbol{x}}(k+1|k) = \boldsymbol{A}\hat{\boldsymbol{x}}(k|k) + \boldsymbol{B}\boldsymbol{u}(k) \tag{14}$$
$$\hat{\boldsymbol{y}}(k|k-1) = \boldsymbol{C}_y\hat{\boldsymbol{x}}(k|k-1)$$

Substituting the third equation of (14) into the first, then eliminating the $\hat{\boldsymbol{x}}(k|k)$ yields

$$\hat{\boldsymbol{x}}(k+1|k) = \boldsymbol{A}\big(\boldsymbol{I} - \boldsymbol{K}_f^T\boldsymbol{C}_y\big)\hat{\boldsymbol{x}}(k|k-1) + \boldsymbol{B}\boldsymbol{u}(k) + \boldsymbol{A}\boldsymbol{K}_f^T\boldsymbol{y}(k) \tag{15}$$

$$= \left(A - K_f C_y\right)\hat{x}(k|k-1) + Bu(k) + K_j y(k)$$

where the gain matrix $K_f = AK_f^T$. This system is stable if $\left|A - K_f C_y\right| < 1$.
Defining the state estimator error as $e(k) = x(k) - x(k|k-1)$, then using (13) we get

$$e(k+1) = \left(A - K_f C_y\right)e(k) \tag{16}$$

which indicates that the error converges to zero provided that the observer is stable. The convergence rate is determined by the eigenvalues of $A - K_j C_y$.

Assuming the state and outputs of the plant to be subjected to white noise disturbances with known covariance matrices, say a matrix ξ_w for the covariance matrix of the process noise and a matrix ξ_v for the covariance matrix of the measurement noise, then the gain matrix K_f can be obtained by solving a discrete algebraic Riccati equation. This kind of observer is known as a Kalman filter.

2.11. Error-free Tracking

In real-world scenarios, inaccuracies in modeling and disturbances are inevitable. The linear model described in (10) does not have a direct method to handle these problems. To make the controller practical, it is necessary to address these issues. Controllers are typically designed with integral action, resulting in zero steady-state error. There are numerous ways to achieve integral action in a controller. For instance, for SISO systems, the introduction of integral action is relatively easy. One common technique involves adding an integrator state to the state space model [5].

Nevertheless, the previously mentioned approach does not work well for MPC controllers. Thus, an alternative method is proposed. This paper employs the same technique developed by Åkesson and Hagander [54]. The technique utilizes a disturbance observer to achieve integral action in the MPC formulation. The augmented system model is formulated as follows:

$$\begin{bmatrix} x(k+1) \\ \xi_a(k+1) \\ \xi(k+1) \end{bmatrix} = \begin{bmatrix} A & 0 & B \\ 0 & I & 0 \\ 0 & 0 & I \end{bmatrix} \begin{bmatrix} x(k) \\ \xi_a(k) \\ \xi(k) \end{bmatrix} + \begin{bmatrix} B \\ 0 \\ 0 \end{bmatrix} u(k)$$

$$z(k) = y_z(k) = [C_z \quad 0 \quad 0][x(k)^T \quad \xi_a(k)^T \quad \xi(k)^T]^T \tag{17}$$

$$y_a(k) = [C_a \quad I \quad 0][x(k)^T \quad \xi_a(k)^T \quad \xi(k)^T]^T$$

where $\xi_a(k) \in R^p$, $\xi(k) \in R^m$, $y_z(k) \in R^{p,}$ and $y_a(k) \in R^p$ denote the output disturbance, the input disturbance, the controlled output, and the additional measured output, respectively. In this scenario, it is assumed that the quantity of controlled outputs, $z(k)$, is equivalent to the number of inputs $u(k)$. Furthermore, it is presumed that the controlled variables are included in the set of measured variables.

2.12. Blocking Factors

There are several conditions where it may be beneficial to keep the control signal unchanged for a few consecutive predicted samples. This permits the control horizon to be increased without adding complexity to the OCP. For instance, if enhancing closed-loop performance requires increasing the control horizon, this will also increase the computation time of the OCP. If this is not desirable, one potential solution is to include only every other decision variable in the OCP. As previously stated, this approach assumes that the control signal remains constant over two consecutive sampling times. To accomplish this goal, let us introduce I_u as the predicted sample index set where the control signal can vary. Similarly, we can generalize the prediction horizon. Rather than including all predicted values in the interval $[k \dots k + L_p - 1]$, we could enforce the set I_p as the sample index corresponding to the predicted output values included in the cost function and constraints. Therefore, using the above notation, we can rewrite the cost function in (12) as follows

$$J(k) = \sum_{i \in I_p} \|\hat{z}(k+i|k) - r(k+i|k)\|_{Q(i)}^2 + \sum_{i \in I_u} \|\Delta\hat{u}(k+i|k)\|_{R(i)}^2 \tag{18}$$

To illustrate the blocking factor concept, consider the following example. Let assume that $L_w = 1$, $L_p = 4$, and $I_p = 2$. Then, only samples [1 3 5 7] will be included in the cost function evaluation. Similarly, assume that $L_u = 3$ and $I_u = 2$. Then, it is assumed that at each sample, we have the predicted control signal $\hat{u}(k) = \hat{u}(k+1)$ and $\hat{u}(k+2) = \hat{u}(k+3)$. Only $\hat{u}(k)$ and $\hat{u}(k+2)$ will be calculated. Thus, the computation load can be reduced.

2.13. Model Predictive Control (MPC) Structure

MPC as indicated by its name, is a model-based control strategy. It uses the model to predict the output. Using these predictions, the goal is to find the control sequence that minimizes the cost function that is dependent on those predicted outputs, reference trajectories, and control actions. The MPC strategy is briefly summarized in the following steps [2]:

a. The future outputs, $\hat{\mathbf{z}}(k + i|k)\ for\ i = 1, \dots, L_p$, are computed over the prediction horizon L_p at each sampling time using the linear model of the system, as described in (14). These values of $\hat{\mathbf{z}}(k)$ depend on the past input and output samples and the future control sequence, $\mathbf{u}(k)$.

b. The values of the control signal $\mathbf{U}(k)$ are calculated using an optimization algorithm to minimize the cost function (18). This criterion, usually in the form of a quadratic function, tries to approximate the future outputs to the future reference signal.

c. After optimization, only the first sample of the signal $\mathbf{U}(k)$ is applied to the system. When new measurement data is available, the overall procedure is repeated.

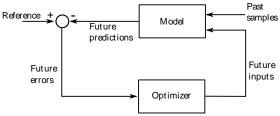The basic structure of an MPC algorithm is given in Fig. 5.

Fig. 5. A basic structure of MPC algorithm.

Many authors proposed various algorithms to solve a constrained case in MPC formulation [2], [5], [55]. The MPC structure for the constrained case is shown in Fig. 6. In this study, the algorithm given in Table 3 is employed. For a detailed description and its implementation in a multivariable system case, one could refer to [56], [57].
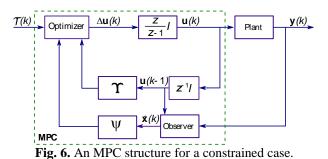

Fig. 6. An MPC structure for a constrained case.

Table 3. An MPC algorithm for constrained case

1: Initialize the MPC tuning parameters ($L_p, L_u, L_w, I_p, I_u, \mathbf{Q}, \mathbf{R}$), the system model matrices ($\mathbf{A}, \mathbf{B}, \mathbf{C}$, and $\mathbf{D}$), and the model prediction matrices ($\mathbf{\Psi}, \Upsilon, \mathbf{\Theta}$).

2: **for** $k = 1{:}L_p, 1{:}L_u - 1$ **do**

  a. Attain the future reference signal $\mathbf{T}(k)$, then calculate the following tracking error matrix:
$$\boldsymbol{\varepsilon}(k) = \mathbf{T}(k) - \mathbf{\Psi}x(k) - \Upsilon\,\mathbf{u}(k-1)$$

  b. Find solutions to QP optimization problems using the active set method.
$$\min_{\Delta U^*(k)} V(k) = const - \Delta \mathbf{U}(k)^T \mathbf{G} + \Delta \mathbf{U}(k)^T \mathbf{H} \Delta \mathbf{U}(k)$$

      subject to

$$\begin{bmatrix} \mathbf{W} \\ \mathbf{F} \\ \mathbf{\Gamma\Theta} \end{bmatrix} \Delta \mathbf{U}(k) \leq \begin{bmatrix} \mathbf{W} \\ -\mathbf{F}\mathbf{u}(k-1) - \mathbf{f} \\ \Gamma[\mathbf{\Psi}x(k + Y\mathbf{u}(k-1) - \mathbf{g})] \end{bmatrix}$$

  c. Calculate the following optimal control input:
$$\mathbf{u}^*(k|k) = [\mathbf{I}_q, \mathbf{O}_q, \dots, \mathbf{O}_q]\Delta \mathbf{U}^*(k) + \mathbf{u}(k-1)$$

  d. Wait for the next sampling time and repeat step **a.**

3: **End**

The tuning parameters for the MPC design are presented in Table 4. The prediction and control horizons are selected by considering the time constants of the linearized system. Choosing too short horizons could result in instability, while too large horizons could lead to increased computational load. Since the smallest and the biggest time constant as defined in (5) are 35.5 s and 116.7 s respectively, then with a sampling time $t_s = 3\ s$, the chosen L_p and L_u as given in Table 4 are reasonable. The horizons correspond to a prediction time of 90 s and a control time of 30 s, respectively. Increasing the horizons without increasing the number of optimization variables can be accomplished by introducing a blocking factor, as previously mentioned. In this particular case, the blocking factor $I_p = I_u = 2$ was specified for control purposes. For further methods on how to tune MPC, one can refer to [58]–[60].

Table 4. Numerical Values of MPC Controller for the QTP

Parameter	Value
L_p	30
L_u	10
L_w	1
I_p	2
I_u	2
$\boldsymbol{Q}$	diag(4, 1)
$\boldsymbol{R}$	diag(0.01, 0.01)
$\boldsymbol{\xi}_w$	diag(1, 1, 1, 1)/diag(1, 1, 1, 1, 1, 1)
$\boldsymbol{\xi}_v$	diag(0.01, 0.01)

Equation (2) indicates that only two states, namely L_1 and L_2, are measurable. This means that there is a need for an observer to estimate the two unknown states, L_3 and L_4. In this study, the Kalman filter, known as an optimal filter [54], will serve as the observer.

3. RESULTS AND DISCUSSION

The control objectives are twofold. Firstly, it is desired to maintain the water levels of the lower tanks (L_1 and L_2) to the given reference levels by manipulating the two pump's voltages. Secondly, the controller must be able to regulate the system response to the setpoint when a constant disturbance comes in. The maximum water level for each tank is 20 cm, which corresponds to 10 V since κ_c is set to 0.5 (refer to Table 1). To ensure a safety margin, the tank level constraints are set at 19.8 cm in this simulation. Specifically, we set $0 \le \boldsymbol{y}(k) \le 19.8$. The pump operations are restricted to 0–10 V, i.e. $0 \le \boldsymbol{u}(k) \le 10$. The control increments $\Delta \boldsymbol{u}(k)$ are also restricted such that $-10 \le \Delta \boldsymbol{u}(k) \le 10$.

It should be noted that the stationary water level of L_2^0 is very near to the maximum level, as indicated in Table 2. Controlling an NMP system that operates close to a constraint is a difficult control problem to resolve. However, by utilizing the MPC algorithm for such a problem, two major advantages of MPC can be demonstrated: the ability to handle multivariable cases and to deal with constraints.

Two cases will be considered in the study. The first case will simulate PID and MPC controllers for a linear NMP model, and the second case will discuss a more realistic scenario using the nonlinear QTP system described in (1) as the plant. For each case, two distinct observers will be considered in MPC designs. The first design (denoted as MPC1 design) will employ a standard Kalman filter, while the second one (denoted as MPC2 design) will use a modified Kalman filter that includes a disturbance model into its integral action formula as expressed in (17). It is worth noting that a disturbance will be applied in both cases to evaluate the performance of the PID and MPC controllers in rejecting disturbances. The tuning parameters for the PID controller are given in (9), while the tuning parameters for the MPC controller are presented in Table 4.

To measure the controller performance, we use integral squared error (ISE), integral absolute error (IAE), and, integral time absolute error (ITAE) as follows

$$ISE = \int_0^{t_f} e^2(t)\, dt, \quad IAE = \int_0^{t_f} |e(t)|^2 dt, \quad ITAE = \int_0^{t_f} t|e(t)|^2 dt$$

3.1. Control Performance for the Linear Model

The results of the first case simulation are presented in Fig. 7. To evaluate the ability of the PID and MPC to track the set point, the following scenario is conducted: at $t = 60\ s$, a step change in the level set

point L_1 of 6 cm is applied while keeping the level set point L_2 constant. Then, at $t = 1500\ s$, a step change in the level set point L_2 of 2 cm is applied while keeping the level set point L_1 constant.

At time $t \leq 1500\ s$, Fig. 7 shows that there is a strong coupling between L_1 and L_2, but both the PID and MPC controllers can handle this situation quite well by achieving the expected set points. The MPC controllers give better transient responses than the PID since no overshoots are introduced in L_1 control loop. However, the PID gives a faster transient response than the two MPCs. The performance of the MPC1 design deteriorates when a constant disturbance is applied to v_1 at $t = 1000\ s$ (see Fig. 8 for a more obvious picture). On the contrary, both the PID and MPC2 design can handle the input disturbance very well. When there is a step change in L_2 set point at $t = 1500\ s$, both the PID and MPC2 design controllers can steer the system responses to the desired set points, whereas the MPC1 design controller fails. This result proves that the MPC algorithm using a Kalman filter that incorporates an input disturbance model as defined in (17) succeeds in obtaining steady-state error-free tracking.

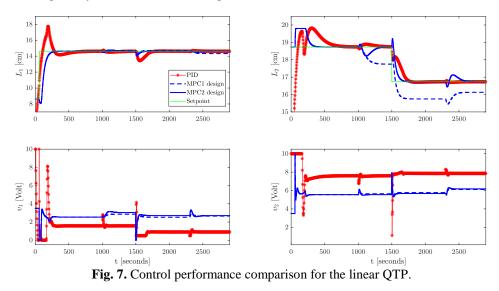**Fig. 7.** Control performance comparison for the linear QTP.

Table. 5 shows that overall the MPC2 design controller gives the smallest error of all the controllers. Again, the numerical results listed in Table. 5 indicate that the proposed MPC method is better than the PID and MPC1 design controllers. It can reduce the overall set point tracking error up to 32.1%, 27.6%, and 38.54% using the performance indices ISE, ITAE, and IAE, respectively, compared to the PID controller.

Table 5. The controller performance comparison for the linear QTP

Control Type	$u - y$	Performance indices		
		ISE	**ITAE**	**IAE**
Decentralized	L_1	382.94	1.364×10^5	245.11
PID	L_2	943.34	1.775×10^5	325.92
MPC1	L_1	760.50	2.257×10^5	253.18
design	L_2	529.6	1.020×10^6	587.24
MPC2	L_1	745.45	5.983×10^4	185.11
design	L_2	155.2	1.675×10^5	165.87

As previously mentioned, the second control objective is that the designed controller must be robust to constant disturbance. Thus, the following scenario is applied to the system: a constant disturbance is introduced to input v_1 at t= 1000 s and to input v_2 at t= 2300 s. The simulation results are given in Fig. 8. Both the PID and MPC2 design can attenuate the input disturbance very well. Unfortunately, the MPC1 design controller– which only employs a standard Kalman filter without input disturbance state– fails to reject the disturbance.

We can conclude from Fig. 7 and Fig. 8 that the designed PID controller can track the set points and reject disturbance quite well since it has been combined with a static decoupler as defined in (9). The decoupler tries to minimize the control loop interaction as small as possible. Additionally, the MPC controller can manage a multivariable system naturally. It can be done by tuning the weight matrices **Q** and **R**.
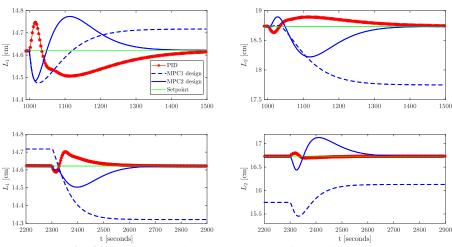
Fig. 8. Disturbance rejection comparison for the linear QTP.

3.2. Control Performance for the Nonlinear Model

In the second case, we use the nonlinear QTP plant model described in (1) to get a more realistic scenario. Both the plant model and PID controller blocks are implemented using Matlab/Simulink, whereas the MPC controller block is represented by an S-function block. The same simulation scenario as in the linear control case is performed and the results are shown in Fig. 9.
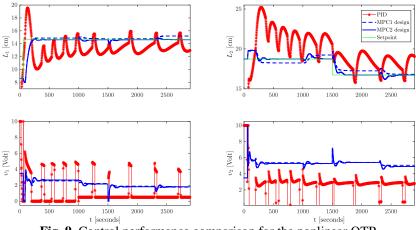

Fig. 9. Control performance comparison for the nonlinear QTP.

Fig. 9 shows both the PID and MPC1 design controllers fail to achieve zero-error tracking even when there are no disturbances. This fact can be understood since a significant model mismatch between the linear and nonlinear QTP exists. Even, the PID controller violates the output constraint for L_2 control loop, i.e. its tank level is over $20\ cm$. It means that the tank L_2 overflows. The degradation in performance of the two controllers is more obvious as listed in Table 6. Again, the MPC2 design controller has superior performance compared to the other controllers. In this case, it can reduce the overall set point tracking error up to 93.4%, 94.9%, and 91.5% using the performance indices ISE, ITAE, and IAE, respectively, compared to the PID controller.

Table 6. The controller performance comparison for the nonlinear QTP

Control Type	$u - y$	Performance indices		
		ISE	ITAE	IAE
Decentralized	L_1	4.17×10^3	1.998×10^6	1.71×10^3
PID	L_2	1.03×10^4	2.74×10^6	2.46×10^3
MPC1	L_1	895.06	4.56×10^5	409.49
design	L_2	1.31×10^4	3.32×10^6	3.09×10^3
MPC2	L_1	807.87	6.284×10^4	191.98
design	L_2	150.3	1.777×10^5	163.61

When an input disturbance is present, only the MPC2 design controller succeeds in achieving zero steady-state error, as seen in Fig. 10. Hence, it can be concluded that the offset-error tracking algorithm is also effective for the nonlinear model.
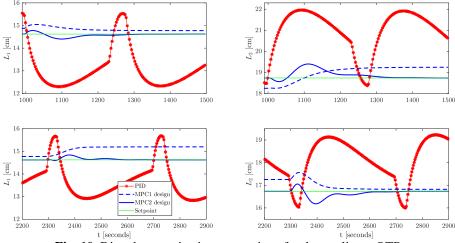

Fig. 10. Disturbance rejection comparison for the nonlinear QTP.

4. CONCLUSION

This article presents an MPC design utilizing the offset-error algorithm to control both the linear and nonlinear quadruple tank process (QTP), a well-known benchmark for control problems. The split ratio of valves γ_i is carefully selected such that a non-minimum phase (NMP) system is obtained. Moreover, the integration of a disturbance observer into the augmented system model within the MPC framework enabled us to achieve error-free tracking, even in the presence of a constant load disturbance. To get more insight, we compare the performance of the proposed MPC algorithm with a conventional decentralized PID and standard MPC.

Our study has demonstrated the practical benefits of the MPC algorithm, including its ability to handle constraints and support multiple input-multiple output (MIMO) systems. Additionally, the proposed offset-error algorithm has proven effective in rejecting load disturbances for both linear and nonlinear QTP models. Compared to the PID control, the proposed method can reduce the overall set point tracking error up to 32.1%, 27.6%, and 38.54% using the performance indices ISE, ITAE, and IAE, respectively, for the linear case. Furthermore, for the nonlinear case, the result is much better. The overall set point tracking error reduction is up to 93.4%, 94.9%, and 91.5% using the performance indices ISE, ITAE, and IAE, respectively.

In alignment with our research objectives, this work highlights the potential of MPC-based control strategies in complex systems like the QTP. The findings presented here open doors to practical applications in industries where precise control and disturbance rejection are critical. Additionally, control of liquid level in tanks and fluid flow between tanks is essential in nearly all process industries such as petrochemical, wastewater treatment, pharmaceutical, food, distillation column, etc. Despite many benefits, MPC also suffers from drawbacks. One of these is that the control law derivation is more complex than that of the classical PID controllers, i.e. MPC needs hardware with high computation power. In case the process dynamic does not change, the derivation of the controller can be done beforehand. However, in the adaptive control case, all the computation has to be carried out online. When any constraints are active, the amount of computation time required is even higher. Fortunately, with the computing power available today, it is not an essential problem anymore.

Future research could explore further refinements to the MPC design, investigate the scalability of the offset-error algorithm to more complex systems, and explore applications in various domains. This study contributes to the ongoing advancement of control systems and offers promising avenues for future research and practical implementation.

REFERENCES

[1] M. Schwenzer, M. Ay, T. Bergs, and D. Abel, "Review on model predictive control: an engineering perspective," *Int. J. Adv. Manuf. Technol.*, vol. 117, no. 5, pp. 1327–1349, 2021, https://doi.org/10.1007/s00170-021-07682-3.

[2] S. V. Raković and W. S. Levine. *Handbook of Model Predictive Control. in Control Engineering*. Cham: Springer International Publishing, 2019, https://doi.org/10.1007/978-3-319-77489-3.

[3] M. B. Saltık, L. Özkan, J. H. A. Ludlage, S. Weiland, and P. M. J. Van den Hof, "An outlook on robust model pre-

dictive control algorithms: Reflections on performance and computational aspects," *J. Process Control*, vol. 61, pp. 77–102, 2018, https://doi.org/10.1016/j.jprocont.2017.10.006.

[4]   P. D. Domański, "Performance Assessment of Predictive Control—A Survey," *Algorithm*s, vol. 13, no. 4, p. 97, 2020, https://doi.org/10.3390/a13040097.

[5]   G. Pannocchia and W. P. Heath, "Offset-free IMC with generalized disturbance models," *Automatica*, vol. 122, p. 109270, 2020, https://doi.org/10.1016/j.automatica.2020.109270.

[6]   S. Ntouskas, H. Sarimveis, and P. Sopasakis, "Model predictive control for offset-free reference tracking of fractional order systems," *Control Eng. Pract.*, vol. 71, pp. 26–33, 2018, https://doi.org/10.1016/j.conengprac.2017.10.010.

[7]   G. Pannocchia and J. B. Rawlings, "Disturbance models for offset-free model-predictive control," *AIChE J.*, vol. 49, no. 2, pp. 426-437, 2003, https://doi.org/10.1002/aic.690490213.

[8]   A. W. Hermansson and S. Syafiie, "An offset-free MPC formulation for nonlinear systems using adaptive integral controller," *ISA Trans.*, vol. 91, pp. 66–77, 2019, https://doi.org/10.1016/j.isatra.2019.01.037.

[9]   K. H. Johansson, "The quadruple-tank process: A multivariable laboratory process with an adjustable zero," I*EEE Trans. Control Syst. Technol.,* vol. 8, no. 3, pp. 456–465, 2000, https://doi.org/10.1109/87.845876.

[10]   L. Pedroso and P. Batista, "Reproducible low-cost flexible quadruple-tank process experimental setup for control educators, practitioners, and researchers," *J. Process Control,* vol. 118, pp. 82–94, 2022, https://doi.org/10.1016/j.jprocont.2022.08.010.

[11]   P. Segovia, V. Puig, E. Duviella, and L. Etienne, "Distributed model predictive control using optimality condition decomposition and community detection," *J. Process Control,* vol. 99, pp. 54–68, 2021, https://doi.org/10.1016/j.jprocont.2021.01.007.

[12]   K. Zare, M. Shasadeghi, T. Niknam, M. H. Asemani, and S. Mobayen, "Constrained Robust Control by a Novel Dynamic Sliding Mode Surface," *Int. J. Control. Autom. Syst.,* vol. 20, no. 3, pp. 823 – 830, 2022, https://doi.org/10.1007/s12555-020-0418-5.

[13]   M. Nagarajapandian, B. Sharmila, S. Kanthalakshmi, and T. Anitha, "Reconfigurable controller design for based controllers used in multivariable methods," *J. Adv. Res. Dyn. Control Syst.*, vol. 11, no. 11, pp. 612–620, 2019, https://doi.org/10.5373/JARDCS/V11SP11/20193074.

[14]   S. R. Mahapatro, B. Subudhi, and S. Ghosh, "Design and experimental realization of a robust decentralized PI controller for a coupled tank system," *ISA Trans.,* vol. 89, pp. 158–168, 2019, https://doi.org/10.1016/j.isatra.2018.12.003.

[15]   S. K. Pandey, J. Dey, and S. Banerjee, "Modified Kharitonov Theorem Based Optimal PID Controller Design for MIMO Systems," *J. Electr. Eng. Technol.*, vol. 18, no. 3, pp. 2317–2334, 2023, https://doi.org/10.1007/s42835-022-01329-3.

[16]   J.-C. Jeng and M.-W. Lee, "Multi-loop PID controllers design with reduced loop interactions based on a frequency-domain direct synthesis method," *J. Franklin Inst.,* vol. 360, no. 4, pp. 2476–2506, 2023, https://doi.org/10.1016/j.jfranklin.2023.01.002.

[17]   K. R. A. Govind, S. Mahapatra, and S. R. Mahapatro, "Design of an Optimal Control Strategy for Coupled Tank Systems Using Nonlinear Constraint Optimization With Kharitonov-Hurwitz Stability Analysis," *IEEE Access,* vol. 11, pp. 72618–72629, 2023, https://doi.org/10.1109/ACCESS.2023.3294109.

[18]   T. Hägglund, S. Shinde, A. Theorin, and U. Thomsen, "An industrial control loop decoupler for process control applications," *Control Eng. Pract.,* vol. 123, p. 105138, 2022, https://doi.org/10.1016/j.conengprac.2022.105138.

[19]   A. Srivastava and L. B. Prasad, "A comparative performance analysis of decentralized PI and model predictive control techniques for liquid level process system," *Int. J. Dyn. Control,* vol. 10, no. 2, pp. 435–446, 2022, https://doi.org/10.1007/s40435-021-00814-3.

[20]   S. R. Mahapatro and B. Subudhi, "A Robust Stability Region-Based Decentralized PI Controller for a Multivariable Liquid Level System," *IEEE Syst. J.,* vol. 16, no. 1, pp. 124–131, 2022, https://doi.org/10.1109/JSYST.2021.3079293.

[21]   K. A. Sundari and P. Maruthupandi, "Optimal Design of PID Controller for the analysis of Two Tank System Using Metaheuristic Optimization Algorithm," *J. Electr. Eng. Technol.,* vol. 17, no. 1, pp. 627–640, 2022, https://doi.org/10.1007/s42835-021-00891-6.

[22]   R. Arivalahan, P. Tamilarasan, and M. Kamalakannan, "Liquid level control in two tanks spherical interacting system with fractional order proportional integral derivative controller using hybrid technique: A hybrid technique," *Adv. Eng. Softw.*, vol. 175, p. 103316, 2023, https://doi.org/10.1016/j.advengsoft.2022.103316.

[23]   J. Arunshankar, "Control of nonlinear two-tank hybrid system using sliding mode controller with fractional-order PI-D sliding surface," *Comput. Electr. Eng.,* vol. 71, pp. 953–965, 2018, https://doi.org/10.1016/j.compeleceng.2017.10.005.

[24]   G. Gurumurthy and D. K. Das, "An $FO\text{-}{{I}^{\lambda }}{{D}^{1-\lambda }}$ controller design and realization for inverted decoupled Two Input Two Output-Liquid Level System," *Int. J. Dyn. Control,* vol. 8, no. 3, pp. 1013–1026, 2020, https://doi.org/10.1007/s40435-019-00602-0.

[25]   A. Numsomran, T. Trisuwannawat, and V. Tipsuwanporn, "Adaptive fractional order PIλDμ control for multi-configuration tank process (MCTP) toolbox," *Int. J. Intell. Eng. Syst.,* vol. 11, no. 5, pp. 21–35, 2018, https://doi.org/10.22266/IJIES2018.1031.03.

[26]   M. Arıcı and T. Kara, "Improved Adaptive Fault-Tolerant Control for a Quadruple-Tank Process with Actuator

Faults," *Ind. Eng. Chem. Res.*, vol. 57, no. 29, pp. 9537–9553, 2018, https://doi.org/10.1021/acs.iecr.8b00817.

[27] X. Meng, H. Yu, J. Zhang, T. Xu, H. Wu, and K. Yan, "Disturbance Observer-Based Feedback Linearization Control for a Quadruple-Tank Liquid Level System," *ISA Trans.,* vol. 122, pp. 146–162, 2022, https://doi.org/10.1016/j.isatra.2021.04.021.

[28] X. Meng, H. Yu, J. Zhang, T. Xu, and H. Wu, "Liquid Level Control of Four-Tank System Based on Active Disturbance Rejection Technology," *Measurement*, vol. 175, p. 109146, 2021, https://doi.org/10.1016/j.measurement.2021.109146.

[29] X. Meng, H. Yu, J. Zhang, and K. Yan, "Optimized control strategy based on EPCH and DBMP algorithms for quadruple-tank liquid level system," *J. Process Control*, vol. 110, pp. 121–132, 2022, https://doi.org/10.1016/j.jprocont.2021.12.008.

[30] X. Meng, H. Yu, T. Xu, and H. Wu, "Disturbance Observer and L2-Gain-Based State Error Feedback Linearization Control for the Quadruple-Tank Liquid-Level System," *Energies,* vol. 13, no. 20. 2020. https://doi.org/10.3390/en13205500.

[31] J. W. S.-Porco, "Low-Gain Stability of Projected Integral Control for Input-Constrained Discrete-Time Nonlinear Systems," *IEEE Control Syst. Lett.,* vol. 6, pp. 788–793, 2022, https://doi.org/10.1109/LCSYS.2021.3086682.

[32] H. Gouta, S. Hadj Saïd, A. Turki, and F. M'Sahli, "Experimental sensorless control for a coupled two-tank system using high gain adaptive observer and nonlinear generalized predictive strategy," *ISA Trans.*, vol. 87, pp. 187–199, 2019, https://doi.org/10.1016/j.isatra.2018.11.046.

[33] B. Gurjar, V. Chaudhari, and S. Kurode, "Parameter estimation based robust liquid level control of quadruple tank system — Second order sliding mode approach," J. Process Control, vol. 104, pp. 1–10, 2021, https://doi.org/10.1016/j.jprocont.2021.05.009.

[34] A. Hosokawa, Y. Mitsuhashi, K. Satoh, and Z.-J. Yang, "Output feedback full-order sliding mode control for a three-tank system," *ISA Trans.*, vol. 133, pp. 184–192, 2023, https://doi.org/10.1016/j.isatra.2022.06.038.

[35] K. Zare, M. Shasadeghi, A. Izadian, T. Niknam, and M. H. Asemani, "Fuzzy modeling and control of a class of non-differentiable multi-input multi-output nonlinear systems," *Asian J. Control,* vol. 24, no. 2, pp. 942–955, 2022, https://doi.org/10.1002/asjc.2530.

[36] D. H. Shah and D. M. Patel, "Design of sliding mode control for quadruple-tank MIMO process with time delay compensation," *J. Process Control,* vol. 76, pp. 46–61, 2019, https://doi.org/10.1016/j.jprocont.2019.01.006.

[37] I. O. Aksu and R. Coban, "Sliding mode PI control with backstepping approach for MIMO nonlinear cross-coupled tank systems," *Int. J. Robust Nonlinear Control,* vol. 29, no. 6, pp. 1854–1871, 2019, https://doi.org/10.1002/rnc.4469.

[38] S. Emebu, M. Kubalčík, C. J. Backi, and D. Janáčová, "A comparative study of linear and nonlinear optimal control of a three-tank system," *ISA Trans.*, vol. 132, pp. 419–427, 2023, https://doi.org/10.1016/j.isatra.2022.06.002.

[39] A. Patel and J. Patel, "LabMIMO: An Open-source Virtual Laboratory for Process Control," *J. Eng. Educ. Transform.,* vol. 36, no. 1, 2022, https://doi.org/10.16920/jeet/2022/v36i1/22142.

[40] P. Navrátil, L. Pekař, and R. Matušů, "Control of a Multivariable System Using Optimal Control Pairs: A Quadruple-Tank Process," *IEEE Access,* vol. 8, pp. 2537–2563, 2020, https://doi.org/10.1109/ACCESS.2019.2962302.

[41] N. N. Son, "Level Control of Quadruple Tank System Based on Adaptive Inverse Evolutionary Neural Controller," *Int. J. Control. Autom. Syst.,* vol. 18, no. 9, pp. 2386 – 2397, 2020, https://doi.org/10.1007/s12555-019-0504-8.

[42] M. A. Eltantawie, "Decentralized neuro-fuzzy controllers of nonlinear quadruple tank system," *SN Appl. Sci.*, vol. 1, no. 1, p. 39, 2019, https://doi.org/10.1007/s42452-018-0029-4.

[43] B. J. Pandian and M. M. Noel, "Control of constrained high dimensional nonlinear liquid level processes using a novel neural network based Rapidly exploring Random Tree algorithm," *Appl. Soft Comput.*, vol. 96, p. 106709, 2020, https://doi.org/10.1016/j.asoc.2020.106709.

[44] A. Jegatheesh and C. A. Kumar, "Novel fuzzy fractional order PID controller for non linear interacting coupled spherical tank system for level process," *Microprocess. Microsyst.*, vol. 72, p. 102948, 2020, https://doi.org/10.1016/j.micpro.2019.102948.

[45] P. C. Blaud, P. Chevrel, F. Claveau, P. Haurant, and A. Mouraud, "From multi-physics models to neural network for predictive control synthesis," *Optim. Control Appl. Methods,* vol. 44, no. 3, pp. 1394–1411, 2023, https://doi.org/10.1002/oca.2845.

[46] N. Rajasekhar, K. K. Nagappan, T. K. Radhakrishnan, and N. Samsudeen, "Application of recurrent neural networks for modeling and control of a quadruple-tank system," *Adv. Control Appl.,* 2023, https://doi.org/10.1002/adc2.158.

[47] M. Nagarajapandian and S. Kanthalakshmi, "Hybrid Optimization of Controller for Multi-variable System," *J. Electr. Eng. Technol.*, pp. 1-13, 2023, https://doi.org/10.1007/s42835-023-01605-w.

[48] I. M. Chew, F. H. Juwono, and W. K. Wong, "GA-Based Optimization for Multivariable Level Control System: A Case Study of Multi-Tank System," *Eng. J.,* vol. 26, no. 5, pp. 25–41, 2022, https://doi.org/10.4186/ej.2022.26.5.25.

[49] A. Osman *et al.*, "Disturbance Observer-Based Feedback Linearization Control for a Quadruple-Tank Liquid Level System," *J. Process Control,* vol. 89, no. 2, pp. 11296–11308, 2022, https://doi.org/10.1016/j.isatra.2021.01.022.

[50] I. A. Oyehan, A. S. Osunleke, and O. O. Ajani, "Closed-Loop Stability of a Non-Minimum Phase Quadruple Tank System Using a Nonlinear Model Predictive Controller with EKF," *ChemEngineering,* vol. 7, no. 4, 2023, https://doi.org/10.3390/chemengineering7040074.

[51] R. G. de S. Câmara and T. L. M. Santos, "Robust decoupling MPC for linear systems with bounded disturbances," *ISA Trans.,* vol. 139, pp. 1–12, 2023, https://doi.org/10.1016/j.isatra.2023.05.004.

[52] I. Kasiyanto, "Advanced Control for Hammerstein-bilinear HVAC System," *in Proceedings of theInternational Conference on Computer, Control, Informatics and Its Applications,* p. 5, 2022, https://doi.org/10.1145/3575882.3575893.

[53] S. A. Frank, "Model Predictive Control," *in SpringerBriefs in Applied Sciences and Technology,* pp. 91–94, 2018, https://doi.org/10.1007/978-3-319-91707-8_12.

[54] J. Akesson and P. Hagander, "Integral action — A disturbance observer approach," *in European Control Conference (ECC)*, pp. 2577–2582, 2003, https://doi.org/10.23919/ECC.2003.7085354.

[55] M. M. Morato, J. E. Normey-Rico, and O. Sename, "Model predictive control design for linear parameter varying systems: A survey," *Annu. Rev. Control*, vol. 49, pp. 64–80, 2020, https://doi.org/10.1016/j.arcontrol.2020.04.016.

[56] I. Kasiyanto, "Design of Hammerstein-Bilinear Model Based Predictive Controller for HVAC Systems," *University of Indonesia*, 2021, https://doi.org/10.13140/RG.2.2.21656.88325.

[57] J. M. Maciejowski. *Predictive Control with Constraints*. Prentice Hall, 2002, https://books.google.co.id/books/about/Predictive_Control.html?id=HV_Y58c7KiwC&redir_esc=y.

[58] C. Ionescu, D. Copot, "Hands-on MPC tuning for industrial applications," *Bull. POLISH Acad. Sci.*, vol. 67, no. 5, pp. 925–945, 2019, https://doi.org/10.24425/bpasts.2019.130877.

[59] R. Nebeluk and M. Ławryńczuk, "Tuning of Multivariable Model Predictive Control for Industrial Tasks," *Algorithms,* vol. 14, no. 1, p. 10, 2021, https://doi.org/10.3390/a14010010.

[60] M. Alhajeri and M. Soroush, "Tuning Guidelines for Model-Predictive Control," *Ind. Eng. Chem. Res.,* vol. 59, no. 10, pp. 4177–4191, 2020, https://doi.org/10.1021/acs.iecr.9b05931.